MATHEMATICAL MODELING AND NUMERICAL SIMULATION FOR MYCOBACTERIUM ULCERANS TISSUE INVASION: A MACROSCOPIC MODEL FOR THE BURULI ULCER DISEASE

[1]PETER ROMEO NYARKO, [2]ISHMAEL JESSE NARH ADIKORLEY, [3]PETER AMOAKO-YIRENKYI, [4]ISAAC K. DONTWI

[1,3,4]Kwame Nkrumah University of Science and Technology (KNUST), Kumasi, Ghana
[2]National Institute of Mathematical Sciences (NIMS), KNUST, Kumasi, Ghana.
E-mail: [1]prnyarko.cos@knust.edu.gh

Abstract- Buruli ulcer (BU) is a neglected, devastating tropical disease necrotizing skin and soft tissue and caused by infection with Mycobacterium ulcerans. The exact mode of transmission is still unknown, but the disease is believed to be transmitted by insect bites, preponderantly in the proximity of rivers, wetlands, and swamps. The bacteria M. ulcerans exude a polyketide lipid toxin, (mycolactone) that causes necrosis to skin and soft tissues and the formation of large ulcers. Understanding the etiology of the disease is very important for the treatment of BU. In this paper a mathematical model of the reaction-diffusion type is developed to account for the macroscopic effect of mycolactone diffusion on cell density, ECM fiber density, and the bacteria population. We numerically solve the coupled system of equations to illustrate tissue invasion with respect to the mycolactone diffusion, M. ulcerans growth, ECM fiber degradation and decrease in cell density in the tissue space as time evolves. The model predicts the extent of tissue invasion and can be used to guide surgery.

Keywords- Buruli ulcer, Mycolactone, Mycobacterium ulcerans, Nonstandard finite difference, Reaction-diffusion equation.

Introduction

Buruli ulcer (BU) is a tropical disease caused by infections with Mycobacterium ulcerans (M. ulcerans) and it affects the skin and soft tissues [1]. It has been recently reported in some countries as the second most prevalent mycobacteriosis in humans after tuberculosis and leprosy [1, 2,3], Higher incidence of the BU disease occurs in tropical regions of Western and Central Africa, but it also exist in North America, the Western Pacific, Australia and China [3] (WHO fact sheet, February 2016). Knowledge about the disease among the public is limited and the mode(s) of transmission is still unknown, but the disease is believed to be transmitted by insect bites, preponderantly in the proximity of rivers, wetlands, and swamps [3]. The disease can affect all age groups, but most cases occur in young patients under the age 15, thus having huge social impact [4]. Complicated cases require between three to eighteen months hospitalization with a significant psychological burden for the patient [4,5]. In Ghana, studies show about 6000 reported BU cases and all 10 regions of the country are affected with the Ashanti region recording the highest percentage [5]. In spite of these facts and of its long history, BU has been largely neglected until recently. The reasons are manifold, but one of the main causes is, it's typical occurrence in rural communities with little economic or political influence and with poor healthcare and the absence of potentially profitable market to attract investment in drug and vaccine development or in research to improve healing prospects [3, 6].

The BU lesions typically manifest as painless and feverless subcutaneous nodules, oedema, plaques, oedematous forms and ulcers prevalently on limbs. The patient is usually systemically well, which may explain deferment in seeking assistance especially in rural regions lacking medical centers. If untreated the swellings evolve into necrotic skin ulcers with deeply undermined edges which often result in scarring and contractual deformities, occasionally also affecting bones, thus causing amputations and severe disabilities [6, 7]. Provisional treatment guidelines recommend the use of selected antimycobacterial drugs (eg. Azithromycin, rifampicin, streptomycin, rifabutin, and clarithromycin) usually combined with surgery [3,8]. The success of the treatment depends, however, on the correct assessment of resection margins, which can be very difficult due to the diffuse spreading of the lesions exhibiting the mentioned undermined edges. Indeed, very high recurrence rates have been reported [9] possibly due to the high diffusivity of M. ulcerans deep into the macroscopically healthy-looking tissue; it is extremely difficult to measure the actual extent of infection in order to determine excision margins during surgery.

In the pathogenesis of BU disease, once M. ulcerans enters the subcutaneous tissue, the organism proliferates and elaborates mycolactone toxin that has affinity for fat cells. The resulting apoptosis and necrosis then provides a favorable environment for further proliferation of the organism. Cells migrate/ diffuse through surrounding tissues towards blood vessels and distal organs in response to a chemoattractant (or chemorepellent) concentration in a process called chemotaxis. Furthermore, cells need to adhere to the extracellular matrix (ECM) fibers in order to be able to move [10]. Mycolactone is diffusible, it degrade collagen in ECM [13,15] and has affinity for cells; therefore the cells will migrate

from a region of low concentration of relevant adhesive molecules to an area with a higher concentration, a process called haptotaxis [11]. The contacts of mycolactone and its surroundings initiate the ulcer.

In this study we use mathematical modeling and numerical simulations to make predictions about tissue degradation by mycolactone (a toxin produced by M. ulcerans) and hence guide surgery. Generally, mathematical modeling open the way for investigating highly complex biomedical aspects whose study in vivo would be potentially unethical and/or extremely expensive (if at all possible). The mathematical model modules involve partial differential equations (PDEs) of the reaction-diffusion-taxis (RDT) type and describe time space dynamics of bacteria and normal cells as well as degradation of extra cellular matrix (ECM) fiber densities in conjunction with a PDE for the mycolactone leading to the structural change in the nodules evolving into open wounds. The problem is conceptually related to wound healing and tumor development and invasion into the surrounding tissue. The pathogenesis of BU infection is believed to be toxin mediated and M. ulcerans is seen as extracellular cluster within areas of necrosis that extend some distant from the site of infection [3, 12]. The toxin is cytotoxic and has local immunosuppressive properties.

At present, the authors found no mathematical model in the literature that models the BU disease as we discuss in this work, but there exist SIR models to show the effects of environmental factors in the development of the disease but not the extent of tissue invasion as we discuss in this study, See [12, 13, 14].

1. Model Formulation

We denote by $b(x,t)$ the density of M. ulcerans, by $c(x,t)$ the density of normal cells, and by $v(x,t)$ and $m(x,t)$ the density of ECM fibers and the concentrations of mycolactone respectively. A necessary factor for diffusion is the existence of concentration gradient, and for the sake of completeness we recall here the Fickian diffusion, which states that the flux, (J_{random},) of material, (which in our case are the densities of M. ulcerans, cells, and the mycolactone toxin) is proportional to the gradient of the concentration of the material. Thus in one dimension, the diffusion of M. ulcerans is given by:

$$J_{random} \propto -\frac{\partial b}{\partial x} \rightarrow J_{random} = -D_b \frac{\partial b}{\partial x}. \quad (2.1)$$

where D_b is the bacterial diffusion coefficient. It is reported that once M. ulcerans gets into the subcutaneous tissue, the organism proliferates and elaborates the mycolactone toxin that has affinity for fat cells. The interaction of mycolactone toxin with the cells results in cell death [3,15]. M. ulcerans then feed on lipids from the necrotic cell for further proliferation, therefore in the bacterial evolution equation the term $J_{\text{chemotaxis}} = \chi(c) b \nabla c$ is the chemotactic response of the bacteria to a chemoattractant secreted by necrotic cell, where $\chi(c)$ is a chemotactic function to illustrate the dependence of the M. ulcerans on the cells. There is competition for tissue space by the bacteria, cell and the ECM fibers. This is modeled by the last term on the right side of first the equation in (2.2). The K_c and K_v denote the carrying capacities of the cell and ECM fibers respectively. The birth rate and carrying capacity of M. ulcerans is given by λ_b and K_b respectively with the parameters a_{12} and a_{13} measuring the competitive effect of c on b and v on b respectively.

The production of mycolactone toxin by M. ulcerans is modeled next with the first term on the right side of the second equation (2.2) being the diffusion term. The production rate $(\zeta(b))$ depends on the M. ulcerans density, at a rate γ_m and with a simple decay term to account for the body's response against the toxin.

We denote the diffusion constant, production and decay rates by D_m, γ_m and λ_m respectively.

The ECM fibers do not diffuse but rather degraded at the rate δ_v through the interaction of mycolactone with collagen fiber which forms the major component of ECM fibers [17]. Furthermore, ECM fibers remodel and reestablish themselves with a production rate λ_v whiles competing for space with the cells and M. ulcerans. The parameters a_{31} and a_{32} measure the competitive effect of b on v and c on v respectively. These considerations lead to the third equation in (2.2).

Mycolactone has been studied extensively for its cytotoxic effects on cells and it has been established that it is the necessary and sufficient virulence factor for BU disease. It causes extensive necrosis and tissue damage and induces apoptotic cell death (mycolactone binding with Wiskott -Aldrich syndrome protein in the cytoplasm of the cell causes cell death). We model the influence of mycolactone on the haptotatic and chemotactic response of cells with the functions $\rho(v)$ and $\psi(c,m)$ respectively. These two functions illustrate the dependence of cell movements on its direct neighbors and surroundings. The second and third terms of the fourth equation in equation (2.2) models the cell flux due to spatial

gradients of stimulating haptotactic and chemotactic responses respectively. The cells are degraded through interactions with mycolactone at a rate of δ_c with a simple decay term to account for natural death or injury to the cell. The cells diffuses with a diffusion coefficient D_c. Similar to the equations describing the ECM fibers density and M. ulcerans density, there is a competition term in the equation for cell flux. λ_c and K_c are the production rate and carrying capacity of c. The parameters a_{21} and a_{23} measure the competitive effect of b on c and v on c respectively, see [18, 19].

From the events described above on the macroscopic evolution of BU we obtain the system of equations in (2.2) below.

$$\begin{cases} \dfrac{\partial b}{\partial t} = \nabla(D_b \nabla b) - \nabla(\chi(c) b \nabla c) + \lambda_b b\left(1 - \dfrac{b}{K_b} - a_{12}\dfrac{c}{K_c} - a_{13}\dfrac{v}{K_v}\right) \\ \dfrac{\partial m}{\partial t} = D_m \Delta m + \gamma\zeta(b) - \lambda_m m \\ \dfrac{\partial v}{\partial t} = -\delta_v m v + \lambda_v v\left(1 - a_{31}\dfrac{b}{K_b} - a_{32}\dfrac{c}{K_c} - \dfrac{v}{K_v}\right) \\ \dfrac{\partial c}{\partial t} = \nabla(D_c \nabla c) - \nabla(\rho(v) c \nabla c) - \nabla(\psi(c,m) c \nabla m) - \delta_c c m + \\ \qquad \lambda_c c\left(1 - a_{21}\dfrac{b}{K_b} - \dfrac{c}{K_c} - a_{23}\dfrac{v}{K_v}\right) \end{cases} \tag{2.2}$$

in $(0,T)\times\Omega$, where $\Omega \subset R^n$ is a bounded domain with a smooth boundary with $n \in \{1,2,3\}$.

The system of equations (2.2) is supplemented with the boundary and initial conditions, (3.1) and (4.1) respectively.

2. Boundary conditions:

$$\nabla v \cdot \upsilon = \nabla m \cdot \upsilon = \nabla b \cdot \upsilon = \nabla c \cdot \upsilon = 0 \text{ on } (0,T)\times\partial\Omega. \tag{3.1}$$

where υ is the outward unit normal vector on $\partial\Omega$.

3. Initial conditions:

$$\begin{aligned} &c(0,x) = c_0(x), \qquad v(0,x) = v_0(x), \\ &b(0,x) = b_0(x), \\ &m(0,x) = m_0(x),\ t \in (0,T], \quad x \in \Omega. \end{aligned} \tag{4.1}$$

We define the following in the model:

$$\rho(v) = \frac{D_k v}{1+v},\ \psi(c,m) = \frac{D_H}{1+cm},\ \chi(c) = \frac{D_q}{(1+c)^2},\ \zeta(b) = \frac{b^2}{(1+b^2)} \tag{4.2}$$

4. Nondimensionalization

Before we perform the numerical simulations, the proposed model, equation (2.2) is written in terms of dimensionless variables. The variables are rescaled using the following variables:

$$\tilde{m} = \frac{m}{M},\ \tilde{v} = \frac{v}{K_v},\ \tilde{b} = \frac{b}{K_b},\ \tilde{c} = \frac{c}{K_c},\ \tilde{x} = \frac{x}{L},\ \tilde{t} = \frac{t}{T} \tag{5.1}$$

where the reference length scale, the reference time unit, and the reference concentration of mycolactone are given as L, T, and M respectively. Using (4.2) and the transformation (5.1), equation (2.2) is written in dimensionless form as:

$$\begin{cases} \dfrac{\partial \tilde{b}}{\partial \tilde{t}} = \nabla.\left(\tilde{D}_b \nabla \tilde{b}\right) - \nabla.\left(\tilde{D}_q \dfrac{1}{(1+\tilde{c})^2}\tilde{b}\nabla\tilde{c}\right) + \\ \qquad \tilde{\lambda}_b \tilde{b}(1 - \tilde{b} - a_{12}\tilde{c} - a_{13}\tilde{v}) \\ \dfrac{\partial \tilde{m}}{\partial \tilde{t}} = \tilde{D}_m \Delta\tilde{m} + \tilde{\gamma}\dfrac{\tilde{b}^2}{(1+\tilde{b})^2} - \tilde{\lambda}_m \tilde{m}. \\ \dfrac{\partial \tilde{v}}{\partial \tilde{t}} = -\tilde{\delta}_v \tilde{m}\tilde{v} + \tilde{\lambda}_v \tilde{v}(1 - a_{31}\tilde{b} - a_{32}\tilde{c} - \tilde{v}). \\ \dfrac{\partial \tilde{c}}{\partial \tilde{t}} = \nabla.\left(\tilde{D}_c \nabla \tilde{c}\right) - \nabla.\left(\tilde{D}_k \dfrac{\tilde{v}}{(1+\tilde{c})}\tilde{c}\nabla\tilde{v}\right) - \\ \qquad \nabla.\left(\tilde{D}_H \dfrac{1}{1+\tilde{c}\tilde{m}}\tilde{c}\nabla\tilde{m}\right) - \tilde{\delta}_c \tilde{c}\tilde{m} + \\ \qquad \tilde{\lambda}_c \tilde{c}(1 - a_{21}\tilde{b} - \tilde{c} - a_{23}\tilde{v}). \end{cases} \tag{5.2}$$

with dimensionless parameters defined as:

$$\tilde{D}_b = D_b\frac{T}{L^2},\ \tilde{D}_q = D_q\frac{T}{K_c L^2},\ \tilde{\lambda}_b = \lambda_b T,$$

$$\tilde{D}_m = \frac{T}{L^2},\ \tilde{\gamma} = \gamma\frac{T}{M},\ \tilde{\lambda}_m = \lambda_m T,$$

$$\tilde{\delta}_v = \delta_v M T,\ \tilde{\lambda}_v = \lambda_v T,\ \tilde{D}_c = D_c\frac{T}{L^2},$$

$$\tilde{D}_k = D_k\frac{K_v T}{L^2}$$

$$\tilde{D}_H = D_H\frac{T}{K_c L^2},\ \tilde{\delta}_c = \delta \mathrm{MT},\ \tilde{\lambda}_c = \lambda_c T$$

We proceed with equation (5.2) by omitting the tildes for convenience.

5. Numerical results

A 1-D numerical simulation of the dimensionless model (5.2) is performed to investigate the qualitative behavior of the model. The following initial conditions were considered,

$$c(0,x) = \exp\left(\frac{-x^2}{\varepsilon}\right),\ x \in [0,1] \text{ and } \varepsilon > 0,$$

$$v(0,x) = \left(1 - \exp(\frac{-x^x}{\varepsilon})\right),\ x \in [0,1] \text{ and } \varepsilon > 0,$$

(6.1)

$b = 0.03c(0.x)$,

$m(0,x) = \kappa b(0,x),\ \kappa \in [0,1).$

for the cell density, ECM fibers density, M. ulcerans density and mycolactone concentration. We also considered $\varepsilon = 0.01$ and $\kappa = 0.1$ throughout the numerical simulations. The initial space is assumed to be occupied with ECM fibers density and cell density with M. ulcerans occupying 3% of the cell population in the tissue space. The concentration of mycolactone is proportional to the density of M. ulcerans. Finite difference method is used for the discretization of the model. The space interval $[0.1]$ is divided into k parts with $k+1$ nodal points, and the space step Δx. Forward difference is used to discretize ECM density v as seen below resulting in equation (6.2)

$$v_i^{n+1} = \frac{1}{1+\delta_v m_i^n \Delta t}[v_i^n + \Delta t \lambda_v v_i^n (1 - a_{31} b_i^n - a_{32} c_i^n - v_i^n)];$$

$$i = 1,2,3,...k.$$

(6.2)

where n denote the time level.

The diffusion term in the equation for mycolactone evolution is discretized using central difference scheme to obtain equation (6.3).

$$m_i^{n+1} = \frac{1}{1+2R-\Delta t\lambda_m}\left[R(m_{i-1}^{n+1} + m_{i+1}^{n+1}) + m_i^n + \Delta t\gamma \frac{(b_i^n)^2}{(1+(b_i^n)^2)}\right]$$

(6.3)

where $R = \frac{D_m \Delta t}{(\Delta x)^2}$. Let $Q = 1 + 2R - \Delta t\lambda_m$ then equation (6.3) can be written as:

$$-Rm_{i-1}^{n+1} + Qm_i^{n+1} - Rm_{i+1}^{n+1} = m_i^{n+1} + \Delta t\gamma \frac{(b_i^n)^2}{(1+(b_i^n)^2)}$$

for $i = 0,1,2,...k$, (6.4)

leading to a $(k+1)\times(k+1)$ system of equations:

$$\mathbf{A_m m^{n+1} = m^n + u_m^{\tilde{n}}} \quad (6.5)$$

Where $\mathbf{m^{n+1}}$ is the vector containing the values of m for the $k+1$ space nodes at $n+1$ time level, $\mathbf{A_m}$ is the tridiagonal matrix obtained from the FDM discretization and $\mathbf{u_m^{\tilde{n}}}$ is the vector with the entries $\Delta t\gamma \frac{(b_i^n)^2}{(1+(b_i^n)^2)}$, $i = 0,1,2,...k$, where we make use of the updated values v_i^{n+1} found by solving (5.2). In the discretization of the PDEs describing the cell and the M. ulcerans, we use the nonstandard finite difference (NSFD) scheme. The NSFD scheme handles the diffusion, chemaotaxis and haptotaxis functions explicitly as described in [18, 20, 22, 24] and the remaining terms implicitly. The random motility, haptotaxis and chemotaxis coefficient terms are handled explicitly with respect to the cell to obtain:

$$\nabla(D_c \nabla c)|_{x_i} = \frac{1}{2(\Delta x^2)} \sum_{k \in N_k} D_c (c_k^{n+1} - c_i^{n+1});$$

$$\nabla(\varphi(v) c \nabla v)|_{x_i} =$$

$$\frac{1}{2(\Delta x^2)} \sum_{k \in N_k} (\varphi_k^n (v_k^{n+1}) c_k^{n+1} + \varphi_i^n (v_i^{n+1}) c_i^{n+1})(v_k^{n+1} - v_i^{n+1});$$

$$\nabla(\psi(c,m) c \nabla m)|_{x_i} =$$

$$\frac{1}{2(\Delta x^2)} \sum_{k \in N_k} (\psi_k^n (c_k^n, m_k^{n+1}) c_k^{n+1} + \psi_i^n (c_i^n, m_i^{n+1}) c_i^{n+1})(m_k^{n+1} - m_i^{n+1})$$

(6.6)

where $N_k = \{i-1, i+1\}$ is the index set pointing at the direct neighbors of the index node x_i.

Using equation (5.2) and (6.6), the resulting system is thus written as equation (6.7).

$$\mathbf{A_c c^{n+1} = c^n + u_c^{\tilde{n}}} \quad (6.7)$$

where $\mathbf{c^{n+1}}$ is the vector containing the values of c for the $k+1$ space nodes at $(n+1)$-th time level. $\mathbf{A_c}$ is the tridiagonal matrix coming from the FDM discretization and $\mathbf{u_c^{\tilde{n}}}$ is the vector with the entries $\Delta t\lambda_c c_i^n (1 - a_{21} b_i^n - c_i^n - a_{23} v_i^n)$, for $i = 0,1,2,3,...k$. After employing equation (6.6) and going through the same discretization for mycobacterium ulcerans, the resulting system is thus written as:

$$\mathbf{A_b b^{n+1} = b^n + u_b^{\tilde{n}}} \quad (6.8)$$

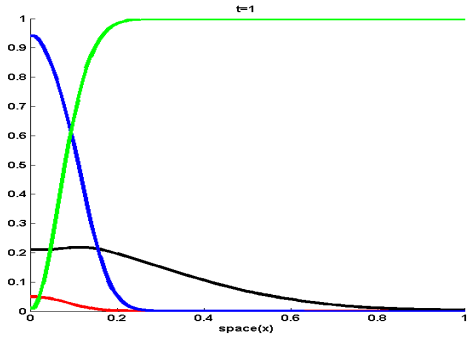
where $\mathbf{b^{n+1}}$ is the vector containing the values of b for the $k+1$ space nodes at $(n+1)$ time level, $\mathbf{A_b}$ is the tridiagonal matrix coming from the FDM

discretization and $\mathbf{U_b^{\tilde{n}}}$ is the vector with the entries $\Delta t \lambda_b b_i^n (1 - b_i^n - a_{12} c_n^n - a_{13} v_i^n)$.

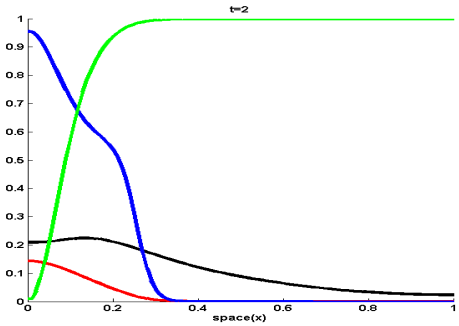
The following parameters were fixed for the numerical simulations

$$D_b = 5\times10^{-5}, \lambda_b = 10^{-3}, D_q = 10^{-3}, a_{12} = 0.2,$$
$$a_{13} = 0.4, D_m = 10^{-2}, \lambda_m = 0.09, \gamma = 0.28,$$
$$\delta_v = 3, \lambda_v = 0.15, a_{31} = 5\times10^{-3}, a_{32} = 3\times10^{-5}$$
$$D_c = 0.1, \delta_c = 2, \lambda_c = 8.5, D_k = 0.03,$$
$$D_H = 10^{-2}, a_{21} = 1.5, a_{23} = 0.9. \qquad (6.9)$$

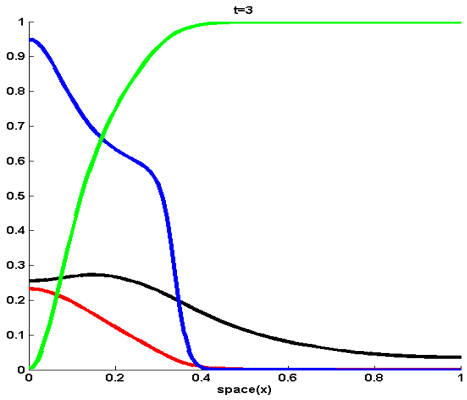
We illustrate the computational results obtained from numerical simulations of the system defined in (5.2). Figure 2. shows the variations of M. ulcerans density (blue), ECM fibers density (green), cell density (black) and mycolactone concentration (red) in space. As can be seen from the plots, as the mycolactone diffuse into the tissue, ECM fibers degrades and there is a decrease in cell density creating space into which the migrating M. ulcerans move. After t =1 through to t =10, the density of M. ulcerans increases as expected. This supports the biological facts mentioned in section 2 that M. ulcerans utilize the fatty acids (lipids) released from dead/ necrotic cells for growth [3]. This is probably why M. ulcerans has often been described as lying in a "pool of lipid". Subsequently, since M. ulcerans produce mycolactone, an increase in the density of M. ulcerans results in an increase in mycolactone concentration as time evolves. The biological implication of the sharp decrease in the concentration of the M. ulcerans may be due to the fact that M. ulcerans dwells in a necrotic focus of the ulcer.



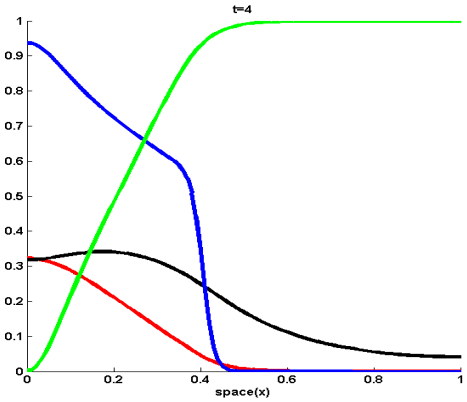
(a)



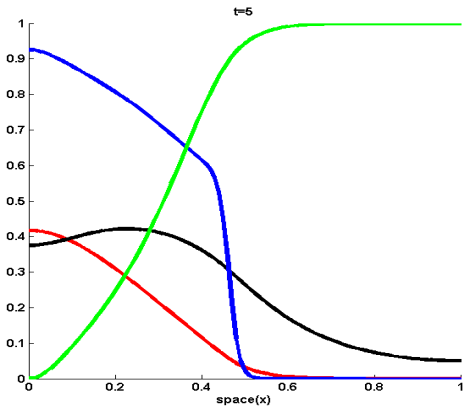
(b)



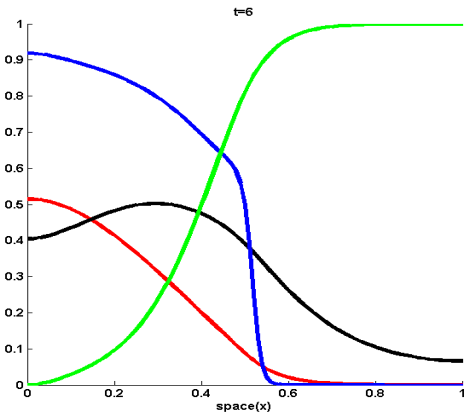
(c)



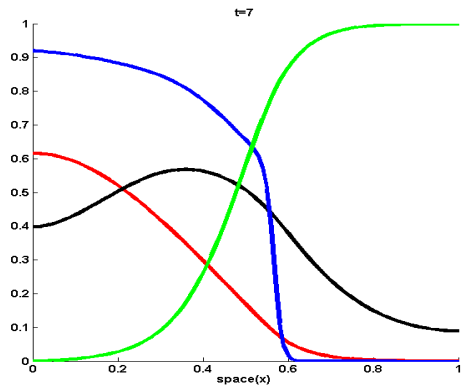
(d)



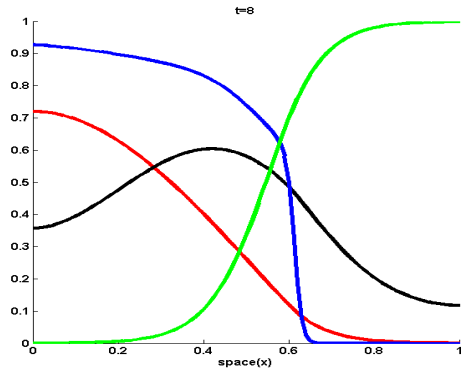
(e)



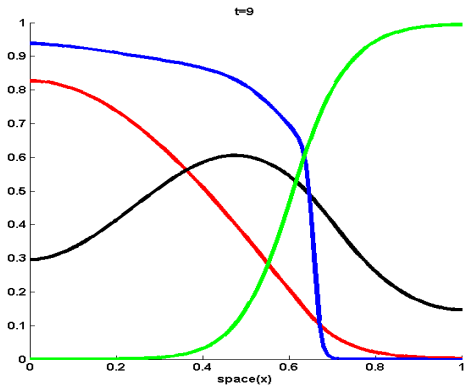
(f)



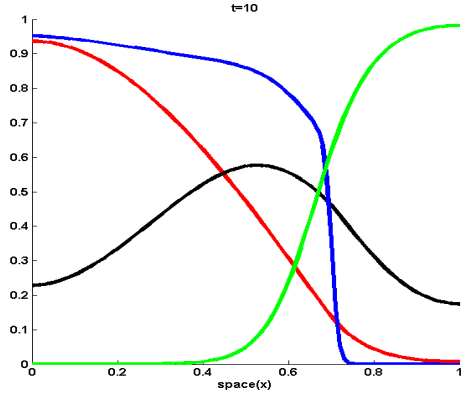
(g)



(h)



(i)

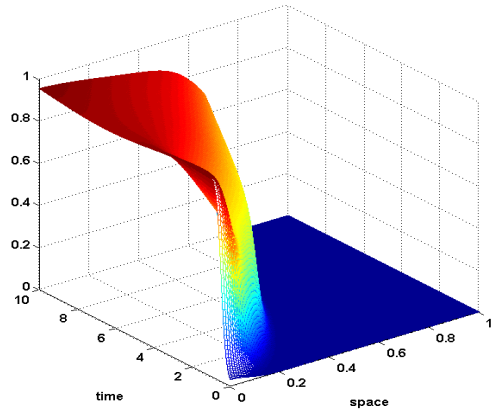


(j)

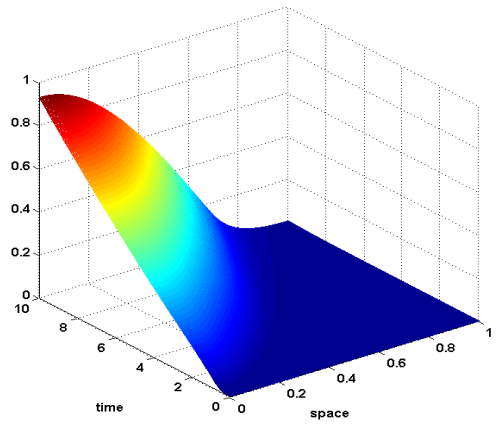
Figure 2: Plots of spatio-temporal evolution of M. ulcerans (blue), the concentrations mycolactone (red), ECM Fibers density (green), and evolution of cell density (black) at time t = 1, 2, 3, 4, 5, 6, 7, 8, 9 and 10.

Notice that after time t=4, the mycolactone diffuses further into the tissue space than the M. ulcerans; this may explain why it is difficult to measure the excision margins during surgery since the toxin diffuses further into the tissue space than the size of the lesion. It may further explain the undermined edges observed in BU disease.

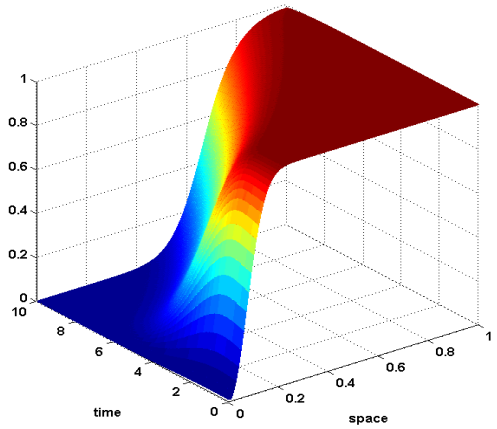
Figure 3. is a 3-D plot showing the evolution M. ulcerans (a), mycolactone concentration (b), ECM fiber density (c) and the cell density (d), for the parameters shown in equation (6.9). This further explains the necrotizing effect of mycolactone on cells as studied in a number of biological experiments [15, 16, 17].



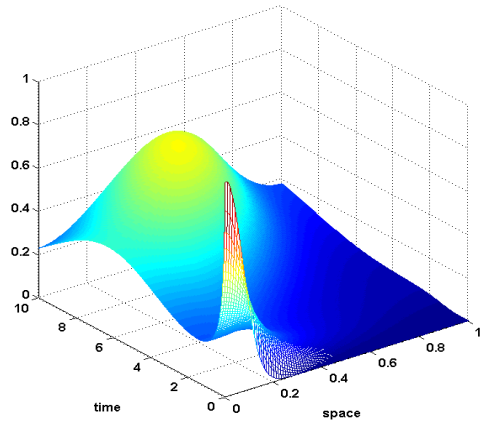
(a) Evolution of Mycobacterium ulcerans



(b) Evolution of mycolactone concentration



(c) Degradation of ECM fibers in space



(d) Evolution of Cell density in space

Figure 3. Evolution in time: M. ulcerans density (a), mycolactone concentration (b), ECM fibers density (c), the normal cell density (d), Solutions at time t=10.

CONCLUSION

In this study we have proposed a mathematical model for M. ulcerans tissue invasion at the macroscopic level. The model consist of a coupled systems of nonlinear partial differential equations describing the interactions between mycolactone , cell density, ECM fibers density, and M. ulcerans M. ulcerans. We used the finite deference scheme to discretize the evolution equations for ECM fibers density and mycolactone concentration. The nonstandard finite difference (NSFD) scheme proposed by R.E. Mickens [21], was used to discretize the evolution equations of M. ulcerans and the cell. The NSFD scheme handles the diffusion, chemotaxis and haptotaxis term explicitly and the remaining terms implicitly. The numerical simulation of the macroscopic model confirms that in the etiology of BU disease, mycolactone (the toxin produced by M. ulcerans) plays a major role in the spread of Buruli ulcer. We also showed the variations of M. ulcerans density, ECM fibers density, cell density and mycolactone concentration in space. The plots for mycolactone concentration and the M. ulcerans density in the tissue space are in sync with the pathology of Buruli ulcer disease at the macroscopic level. M. ulcerans lie in a necrotic focus with the lesion extending some distance from the site of bacterial colonization. The results from the numerical simulations in our model are similar to those from wound healing and tumor development and invasion of tissue [22, 23 24]. Further experimental work is required to validate the parameters in the model. In our next study we develop a multiscale model to include the microscopic level interactions of mycolactone and WASP. To this end the haptotatic and chemotactic functions will depend on these micro-level interactions. The results confirm the cytotoxicity of mycolactone to cells and its degrading effect on ECM. The model can be used to guide surgery.

REFERENCES

[1] [1] WHO, Buruli ulcer : Mycobacterium ulcerans infections, Tech. rep. (2000). http://apps.who.int/iris/bitstream/10665/66164/1/

[2] [2] C. Engwer, A. Hunt, and C. Surulescu, Effective equations for anisotropic glioma spread with proliferation: a multiscale approach, IMA J. Math. Medicine Biol., 2015, doi: 10.1093/imammb/dqv030.

[3] [3] WHO, Buruli ulcer : diagnosis of mycobacterium ulcerans disease: a manual for health care providers,

[4] Tech. rep. (2001).

[5] http://apps.who.int/iris/bitstream/10665/67000/1/

[6] [4] P. Agbenorku, P. Saunderson, Mycobacterium ulcerans Disease of the Face: The Fate of the Victims, J. Mycobac. Dis. 3 (2013), e1000133

[7] [5] P. Agbenorku, Buruli Ulcer Disability in Ghana: The Problems and Solutions, British J. Medicine Med. Res. 4 (2014), 1355-1365.

[8] [6] WHO, Buruli ulcer; fact sheet, (2017), http://www.who.int/mediacentre/factsheets/fs199/en/

[9] [7] P. D. R. Johnson,T. Stinear, P. L. C. Small, G. Plushke, R.W. Merritt, et al. Buruli ulcer (M. ulcerans infection): New insights, new hope for disease control. (2005), PLoS Med 2(4): e108.

[10] [8] R. C. Johnson, M. Makoutod, E. P. Sopoh, G. E. and, J. Gbovi, L. H. Pouteau, W. M. Meyers, M. Boko, F. Portaels, Buruli ulcer distribution in benin, Emerg Infect Disease 11 (3) (2005) doi:10.3201/eid1103.040597

[11] [9] G. Amofah, F. Bonsu, C. Tetteh, J. Okrah, K. Asamoa, K. Asiedu, J. Addy, Buruli ulcer

[12] in ghana: Results of a national case search, Emerging Infectious Diseases 8 (2002) 167-170.

[13] doi:10.3201/eid0802.010119.

[14] [10] J.C. Adams, Regulation of protrusive and contractile cell-matrix contacts, J. Cell Sci.115 (2002), 257-265.

[15] [11] S.B. Carter, Haptotaxis and the mechanism of cell motility, Nature 213 (1967), 256-260.

[16] [12] A. Y. Aidoo, B. Osei, Prevalence of aquatic insects and arsenic concentration determine the geographical distribution of mycobacterium ulcerans infection, Computational and Mathematical Methods in Medicine (8) (2007) 235{244. http://dx.doi.org/10.1080/17486700701695167

[17] [13] T. Lam, R. Smith? A. Kealey, Determining the transmission route of the buruli ulcer using a mathematical model (2012). URL https://www.ruor.uottawa.ca/bitstream/10393/23213/1/LamTiffany2012:pdf

[18] [14] E. Bonyah, I. K. Dontwi, F. Nyabadza, A theoretical model for the transmission dynamics of the buruli ulcer with saturated treatment, Computational and Mathematical Methods in Medicine 2014 (2014) 14 pages. doi:10.1155/2014/576039.

[19] [15] J Clin Invest. 2013;123(4):1501–1512. doi:10.1172/JCI66576

[20] [16] F. Sarfo, R. Phillips et. al. Recent advances: role of mycolactone in the pathogenesis and monitoring of Mycobacterium ulcerans infection/Buruli ulcer disease (2016), 18(1): 17–29, doi: 10.1111/cmi.12547.

[21] [17] J. B. Gama, S. Chimeier, T. G. Martins, et. al., Proteomic analysis of action of the mycobacterium ulcerans toxin mycolactone: Targeting host cell cytoskeleton and collagen. 8(8), (2014), doi: 10.1371/journal.pntd.0003066

[22] [18] G. Meral, C. Stinner, C. Surulescu, On a multiscale model involving cell contractivity and its effect on tumor invasion, Discrete and Continuous Dynamical Systems Serie-B 20 (2015) 189-213.

[23] [19] C Märkl, G. Meral, C. Surulescu, Mathematical analysis and numerical simulations for a system modeling acid-mediated tumor cell invasion, International Journal of Analysis 2013 (2013) 15 pages.doi:10.1155/2013/878051

[24] [20] H. J. Eberl, L. Demaret, A finite difference scheme for a degenerated diffusion equation arising in microbial ecology, Electron. J. Di_erential Equations (2007) 77-96.

[25] [21] R. E. Mickens, Application of nonstandard finite difference schemes. (2005), ISBN 981-256-404-7.

[26] [22] G. Meral, C. Surulescu, Mathematical modelling, analysis and numerical simulations for the influence of heat shock proteins on tumour invasion, J. Math. Anal. Appl (408) (2013) 597-614.

[27] [23] M. Kolev and B. Zubik-Kowal Numerical Solutions for a Model of Tissue Invasion and Migration of Tumour Cells (2011) doi:10.1155/2011/452320

[28] [24] C. Stinner, C. Surulescu, and G. Meral, A multiscale model for pH-tactic invasion with time-varying carrying capacities, IMA J. Appl. Math. 80 (2015) 1300-1321.

★★★